Year: 2011

Myopathy caused by mammalian target of rapamycin complex 1 (mTORC1) inactivation is not reversed by restoring mitochondrial function

Romanino, Klaas and Mazelin, Laetitia and Albert, Verena and Conjard-Duplany, Agnès and Lin, Shuo and Bentzinger, C. Florian and Handschin, Christoph and Puigserver, Pere and Zorzato, Francesco and Schaeffer, Laurent and Gangloff, Yann-Gaël and Rüegg, Markus A.

Originally published as:

Romanino, Klaas and Mazelin, Laetitia and Albert, Verena and Conjard-Duplany, Agnès and Lin, Shuo and Bentzinger, C. Florian and Handschin, Christoph and Puigserver, Pere and Zorzato, Francesco and Schaeffer, Laurent and Gangloff, Yann-Gaël and Rüegg, Markus A.. (2011) *Myopathy caused by mammalian target of rapamycin complex 1 (mTORC1) inactivation is not reversed by restoring mitochondrial function.* Proceedings of the National Academy of Sciences of the United States of America, Vol. 108, H. 51. S. 20808-20813.

The role of mitochondrial activity in the muscle myopathy caused by the inactivation of mTORC1 in skeletal muscle

Klaas Romanino[1], Laetitia Mazelin[3], Verena Albert[1], Agnes Duplany[3], Shuo Lin[1], C. Florian Bentzinger[1, 4], Christoph Handschin[1], Pere Puigserver[2], Laurent Schaeffer[3], Yann-Gaël Gangloff[3] and Markus A. Rüegg[1]

[1]Biozentrum, University of Basel, Basel, 4056, Switzerland
[2]Dana Farber Cancer Institute and Department of Cell Biology, Harvard Medical School, Boston, MA 02115, USA.
[3]Laboratoire de Biologie Moléculaire de la Cellule, Centre National de la Recherche Scientifique, Unité Mixte de Recherche 5239, IFR128, Université de Lyon, Equipe Différenciation Neuromusculaire, Ecole Normale Supérieure, 69364 Lyon Cedex 07, France

Published in Proc Natl Acad Sci U S A. 2011 Dec 20;108(51):20808-13. PMID: 22143799. doi: 10.1073/pnas.1111448109

The role of mitochondrial activity in the muscle myopathy caused by the inactivation of mTORC1 in skeletal muscle

Klaas Romanino[1], Laetitia Mazelin[3], Verena Albert[1], Agnes Duplany[3], Shuo Lin[1], C. Florian Bentzinger[1, 4], Christoph Handschin[1], Pere Puigserver[2], Laurent Schaeffer[3], Yann-Gaël Gangloff[3] and Markus A. Rüegg[1]

[1]Biozentrum, University of Basel, Basel, 4056, Switzerland
[2]Dana Farber Cancer Institute and Department of Cell Biology, Harvard Medical School, Boston, MA 02115, USA.
[3]Laboratoire de Biologie Moléculaire de la Cellule, Centre National de la Recherche Scientifique, Unité Mixte de Recherche 5239, IFR128, Université de Lyon, Equipe Différenciation Neuromusculaire, Ecole Normale Supérieure, 69364 Lyon Cedex 07, France
[4]Present address: The Sprott Centre for Stem Cell Research, Regenerative Medicine Program, Ottawa Health Research Institute, Ottawa, Ontario K1H 8L6, Canada.

Correspondence to:
Markus A. Rüegg, Ph.D.
Biozentrum, University of Basel
Klingelbergstrasse 70
4056 Basel
Switzerland
Phone: +41 61 267 2223
Email: markus-a.ruegg@unibas.ch

SUMMARY

mTOR complex 1 (mTORC1) is central to the control of cell, organ and organismal size. Skeletal muscle-specific inactivation of mTORC1 in mice results in smaller muscle fibers, fewer mitochondria, increased glycogen stores and a progressive myopathy that causes premature death. Interestingly, PGC-1α, which regulates mitochondrial biogenesis and glucose homeostasis, was strongly downregulated. Here we tested whether activation of PGC-1α is sufficient to reverse the phenotype in the mTORC1-inactive mice using a genetic and a pharmacological approach. We show that both paradigms improve mitochondrial function but do not affect the progressive myopathy. In addition, we find that the mTORC1 pathway is dominant over PGC-1α in determining the amount of glycogen stored. Thus, our work provides strong functional evidence that mitochondrial dysfunction in mice with inactivated mTORC1-signaling is due to downregulation of PGC-1α. Importantly, this downregulation does not cause the lethal myopathy and glycogen increase.

Highlights: raptor, PGC-1α, mTOR, bezafibrate,

INTRODUCTION

Adaptations of skeletal muscle to changes in the environment have been shown to depend on insulin-like growth factor (IGF); protein kinase B (PKB)/Akt and mammalian target of rapamycin (mTOR) signaling (Glass, 2005). mTOR is a highly conserved protein kinase that is best known for its central role in the control of cell size through the regulation of protein synthesis (Wullschleger et al., 2006). It is found in two distinct multiprotein complexes, called mTOR complex 1 (mTORC1) and mTORC2. Mice with muscle-specific deletion of *mTOR* or *raptor*, an essential component of mTORC1, suffer from a progressive muscle myopathy that causes premature death at the age between four and six months (Bentzinger et al., 2008; Risson et al., 2009). Importantly, muscles of mTOR^{-} (mTOR muscle knockout) and RAmKO (raptor muscle knockout) mice showed impaired mitochondrial function and an increase in glycogen. The mitochondrial phenotype correlated with the strong reduction of peroxisome proliferator activated receptor-γ (PPARγ) coactivator α (PGC-1α), which regulates mitochondrial biogenesis and glucose homeostasis in skeletal muscle (Wende et al., 2007; Wu et al., 1999) and has been shown to associate with mTOR (Cunningham et al., 2007). Interestingly, like in RAmKO and mTOR^{-} mice, muscle-specific inactivation of *PGC-1α* resulted in a myopathy leading to muscle damage and regeneration (Handschin et al., 2007a) and overexpression of PGC-1α in *mdx* mice, a mouse model of Duchenne muscular dystrophy, was shown to ameliorate the disease phenotype (Handschin et al., 2007b). These data suggest that both, the metabolic (mitochondria and glycogen content) and the myopathic phenotype, of mTOR^{-} and RAmKO mice could be based on the deregulation of PGC-1α expression.

In the current study, we tested this question by transgenic overexpression of PGC-1α in RAmKO mice and by pharmacological activation of PGC-1α by

bezafibrate, a PPAR pan-agonist (Wenz et al., 2008) in mTOR^{-} mice. We find that both treatments improve mitochondrial function but that they do not affect the progressive muscle myopathy. In addition, we find that the increase in glycogen in mTOR^{-} and RAmKO mice is predominated by the activation of PKB/Akt and not by changes in PGC-1α. Thus, while mitochondrial changes in mTOR^{-} and RAmKO mice are functionally linked to the decreased levels of PGC-1α, both the progressive myopathy and the increase in glycogen are not directly associated with those changes.

RESULTS

Transgenic overexpression of PGC-1α restores mitochondrial function in RAmKO mice

One of the most striking phenotypes of RAmKO and mTOR^{-} mice is the decrease in oxidative capacity and the morphological changes in the mitochondria (Bentzinger et al., 2008; Risson et al., 2009). In both mouse models, this correlated with a decrease in the transcript levels of PGC-1α, which led to the hypothesis that the mitochondrial phenotype was due a direct effect of mTORC1 on the expression of PGC-1α, as had been suggested earlier (Cunningham et al., 2007). To test this hypothesis, we therefore crossed RAmKO mice with mice that overexpress PGC-1α in skeletal muscle using the muscle creatine kinase (MCK) promoter (Lin et al., 2002). The resulting RAmKO mice that were also transgenic for PGC-1α (called herein RAmKO-PGC1α-TG) expressed increased levels of PGC-1α in both fast- (Extensor digitorum longus (EDL), Figure 1A) and slow- twitch (soleus, Figure S1A available online) muscles, despite the reduced amount of raptor as shown by Western blot analysis (Figure S1B available online). To evaluate the effect of PGC-1α on mitochondria number, we used quantitative real-time PCR (qRT-PCR) to determine the copy number of mtDNA (D-loop region) relative to the amount of genomic DNA (using sequences for the gene *Ndufv1*) (Amthor et al., 2007). These data showed that RAmKO mice have a reduced number of mitochondria (Figure 1B), consistent with their low oxidative capacity. The reduction of mitochondria was restored to wild-type levels in RAmKO-PGC1α-TG mice, although the mitochondria level was still lower than in the PGC1α-TG mice (Figure 1B). The same trend was seen for transcript encoding mitochondrial proteins, including medium-chain acyl dehydrogenase (MCAD), cytochrome c, cytochrome c oxidase (COX IV), and citrate synthase (Figure

1C), which are all known targets of PGC-1α (Wu et al., 1999). These data thus show that PGC-1α is functional in the RAmKO-PGC1α-TG mice. This was also confirmed by the NADH-tetrazolium (NADH-TR) staining of skeletal muscle as the low oxidative capacity is reversed to at least control levels in RAmKO-PGC1α-TG mice (Figure 1D). The improvement of mitochondria by the overexpression of PGC-1α was also obvious in electron micrographs, which clearly indicate the restoration of both the shape and the number of mitochondria in RAmKO-PGC1α-TG mice. In fact, the size of the mitochondria was increased compared to control like those in muscle from mice transgenic for PGC-1α (Figure 1E; Wende et al., 2007; Wenz et al., 2008).

The mTORC1 and PKB/Akt predominate over PGC-1α on the regulation of glycogen in skeletal muscle

Recent evidence has implicated PGC-1α in the regulation of glucose metabolism in muscle (Wende et al., 2007). As RAmKO and mTOR$^-$ mice had an approximately 5-fold increase in glycogen in skeletal muscle (Bentzinger et al., 2008; Risson et al., 2009), we also investigated whether PGC-1α expression would affect this parameter. To examine this, we stained muscle cross-sections with periodic acid-Schiff (PAS) and quantified the amount of glycogen by an enzymatic assay. As described before (Bentzinger et al., 2008; Wende et al., 2007), the glycogen content was increased in RAmKO and PGC1α-TG mice (Figure 2A and B). The increase in glycogen was much more pronounced in the RAmKO mice than in PGC1α-TG mice. Interestingly, the effect of PGC-1α and raptor deletion was additive (RAmKO-PGC1α-TG mice; Figure 2 A and B), suggesting that the two factors affect independent signaling pathways. One mechanism responsible for the stronger increase of glycogen in RAmKO mice is very likely due to the hyperactivation of PKB/Akt seen by the hyperphosphorylation of the T308 and S473 site of PKB/Akt (Figure 2C, Table 1

available online). An additional observation we made is that the total amount of PKB/Akt is increased when PGC-1α levels are increased (Figure 2C, Table 1 available online). This nevertheless does not seem to have an effect on both phosphorylations of PKB/Akt, as those are unchanged when one compares the *raptor*-deleted mice with the other two mouse models.

A well described target of PKB/Akt is the glycogen synthase kinase 3β (GSK3β), which inhibits the glycogen synthase (Sakamoto and Goodyear, 2002). This protein again was hyperphosphorylated (Figure 2C, Table 1 available online) indicating a higher synthesis of glycogen in the skeletal muscles. The mechanism suggested for the milder increase of glycogen in the PGC1α-TG mice is the downregulation of the glycogen phosphorylase (Wende et al., 2007). This downregulation can be observed in these mice both on the mRNA (Figure 2D) as well as on the protein level (Figure 2C, Table 1 available online). What is striking is that the same could be observed in the two other mouse models. RAmKO mice and PGC1α-TG mice have very different levels of PGC-1α, but in both mouse models the glycogen phosphorylase is down to the same extent.

Increase in PGC-1α expression does not prevent muscle dystrophy in mice with inactive mTORC1

When PGC-1α levels are maintained transgenically, the loss of muscle mass after denervation is reduced and muscle fiber volume is maintained (Sandri et al., 2006). One of the main features of the RAmKO mice was muscle atrophy and a progressive muscle dystrophy resulting in their premature death. Thus an amelioration of the dystrophic phenotype could be expected in the RAmKO-PGC1α mice. Nevertheless when weighing the muscles of 140-day old mice of all our mouse models the reduction of skeletal muscles could still be observed in the RAmKO-PGC1α-TG mice

(Table 2 available online) just as the significant reduction of the whole body weight after 60 days of age (Figure 3A). At an age of 90 days the RAmKO-PGC1α-TG mice showed several signs of a muscle dystrophy in a hematoxylin eosin (H&E) staining of cross-sections (Figure 3B). The mice showed a high number of very small fibers (blue arrows), resulting in an alteration of the muscle size distribution (Figure 3C). Additionally mononuclear cells were found (green arrows), as were centralized nuclei in several muscle fibers (white arrows in Figure 3B and quantification in Figure D). This severe myopathy resulted in a reduced activity of the RAmKO mice that was not significantly changed upon the increase of PGC-1α levels (Figure E). Additionally the mice developed a severe kyphosis after around 20 weeks (Figure 3F and G) and died prematurely (data not shown), again known signs of muscle dystrophy already described in the RAmKO mice (Bentzinger et al., 2008). These results point out that the increase of PGC-1α, although beneficial for the mitochondrial function and number is not sufficient to rescue the dystrophic phenotype of RAmKO mice.

Bezafibrate partially restores mitochondria function in muscles in the absence of mTOR and does not affect the muscle dystrophy

We could show that in mTORC1-inactivated muscles the mitochondrial but not the dystrophic phenotype could be rescued through a genetic increase of PGC-1α. Next we decided to test if a pharmacological approach would show the same results. For this we used bezafibrate, a PPAR pan-agonist that activates the PPARs/ PGC-1α pathway (Bastin et al., 2008; Tenenbaum et al., 2005). Administration of bezafibrate increases PGC-1α expression and its best described targets in skeletal muscle and was shown to improve a mitochondrial myopathy phenotype (Wenz et al., 2008). To see if our observations are consistent in different mouse models, we used mice with a skeletal muscle-specific ablation of *mTOR* (called mTOR^{-}), which show a very

similar phenotype as the RAmKO mice. The mitochondrial function is reduced and the mice suffer from a progressive muscle dystrophy that is more pronounced than the RAmKO mice (Risson et al., 2009). The mTOR$^-$ mice were fed a diet containing 0.5% bezafibrate for 20 weeks starting at 5 weeks of age. qRT-PCR analysis showed that bezafibrate treatment significantly increased expression of PGC-1α and several mitochondrial proteins (Figure 4A). In addition, bezafibrate partially restored the activity of oxidative enzymes as shown by staining muscle cross sections for succinate dehydrogenase- (SDH) and cytochrome oxidase (COX) (Figure 4B; Figure S2B available online). Significantly increased oxidative capacity of mTOR$^-$ muscles was further confirmed by measuring SDH activity directly (Figure 4C).

We next addressed if improved mitochondrial function would ameliorate the muscle dystrophy in the mTOR$^-$ mice. H&E staining of muscle cross sections showed that the signs of muscle dystrophy are still present after the bezafibrate treatment (Figure 4D). In addition, cycles of muscle de- and regeneration were still increased as shown by the increased levels of perinatal muscle myosin heavy chain (MHC) MyH8 and myogenin. Also the levels of dystrophin, which are reduced in mTOR$^-$ mice (Risson et al., 2009), were not affected by bezafibrate (Figure 4E). Moreover, muscle mass was reduced (Table 3 available online), bezafibrate-treated mTOR$^-$ mice develop a kyphosis (Figure S2A available online) and still died around the same age as untreated mice (data not shown). Finally, bezafibrate did not improve specific force production, as the tetanic force (Po) was still reduced in both fast- (tibialis anterioris) and slow- twitch (soleus) muscles of mTOR$^-$ mice (Table 3 available online).

DISCUSSION

This work provides direct functional evidence that the mitochondrial deficits in mTOR$^-$ and RAmKO mice are the consequence of decreased expression of PGC-1α. Furthermore, our study shows that both the high glycogen content and the severe myopathy observed in mTORC1-deficient mice cannot be reversed by changing PGC-1α function. We chose to examine this question by using (1) mice transgenic for PGC-1α (Lin et al., 2002), where the transgene is driven by the MCK promoter that is mainly expressed in fast-twitch muscle fibers and (2) bezafibrate which reaches all muscles. Also, bezafibrate is used in clinical trials and was successfully used in the ∆cox10 mouse model to delay the onset of the mitochondrial myopathy (Wenz et al., 2008). The rescue in mitochondrial number and function is based on the normalization of the mtDNA content, of the levels of key mitochondrial enzymes and of the oxidative capacity. Despite the normalization of the oxidative capacity in RAmKO-PGC1α-TG mice, overall running activity was still much lower than in control mice. This clearly suggests that it is rather the myopathic than the metabolic changes in RAmKO muscle that prevent the mice to run as far as control littermates.

The mechanism by which mTORC1 influences expression of PGC-1α and therefore mitochondrial biogenesis is the formation of a complex of mTORC1, PGC-1α and the transcription factor yin-yang 1 (YY1; Cunningham et al., 2007). Surprisingly, our data now show that the function of PGC-1α to drive mitochondrial biogenesis does not require mTORC1. However, we noted that the expression levels of PGC-1α and its downstream targets, such as MCAD and cytochrome C, were consistently lower in RAmKO-PGC1α-TG than in PGC1α-TG mice. An additional reason for the lower levels of PGC-1α could the increased activity of PKB/Akt in the RAmKO-PGC1α-TG mice. Activated PKB/Akt was shown to directly inhibit PGC-1α by phosphorylation (Li et al., Nature 2007).

We also observed that the genetically modified muscles all contained a 2 to 15-fold increase in glycogen. Our findings that PGC-1α-TG and RAmKO-PGC-1α-TG mice have increased levels of glycogen compared to their respective littermate controls, is in agreement with the finding, that PGC-1α inhibits transcription of glycogen phosphorylase (Wende et al., 2007). However, the increase in glycogen was much more pronounced in those mice deficient for raptor, suggesting that glycogen content is predominantly determined by the activity of mTORC1 and not by PGC-1α. Moreover, in the RAmKO mice, glycogen phosphorylase levels are low despite the low levels of PGC-1α. We hypothesize that this effect on glycogen phosphorylase is due to the strong hyperactivation of PKB/Akt, as was seen in hepatocytes (Aiston et al., 2006). In addition, activated PKB/Akt regulates glycogen synthase via GSK3β (Sakamoto and Goodyear, 2002). Thus, the change in both enzymes is probably responsible for the pronounced increase in glycogen in the raptor-deficient mice.

Finally, our data also show that increased levels of PGC-1α and improved mitochondrial function is not sufficient to reverse any aspects, such as fibrosis, atrophy, centralized nuclei of the severe myopathy in mTORC1-deficient mice. Most importantly, disease onset was not altered at all by the overexpression of PGC-1α or the administration of bezafibrate. We could not observe a beneficial effect of PGC-1α overexpression on muscle mass in the slightly atrophic RAmKO muscle although it has been reported that PGC-1α can counteract denervation-induced atrophy and age-related muscle loss (Sandri et al. 2006; Wenz et al. 2009).

The exact molecular mechanisms responsible for the lethal myopathic phenotype in RAmKO and $mTOR^{-}$ mice remain open. Circumstantial data indicate that the accumulation of glycogen is unlikely the cause. For example, mice overexpressing a hyperactive form of glycogen synthase, which results in a more than 20-fold higher

concentrations of glycogen do not display any muscular dystrophy or change in exercise performance (Pederson et al., 2005).

The most likely scenario is that alteration in the balance between protein synthesis and protein degradation is responsible. Changes in this balance affect proteasomal and autophagic protein degradation and overall protein synthesis. Recent evidence indeed shows that such a shift in the balance results in dystrophic phenotypes, be it via the inactivation of autophagy (Masiero et al., 2009), the proteasome pathway and hyperactivation of PKB/Akt (Grumati et al., 2010). Thus, a change in the balance between protein synthesis and degradation as observed in RAmKO and $mTOR^{-}$ mice is likely to affect the health of skeletal muscle.

In summary, our data show that the mTORC1 regulates mitochondrial activity through PGC-1α and is also the main regulator of glycogen in skeletal muscle. Plus the muscle dystrophy seen after the inactivation of mTORC1 is not dependent on mitochondrial activity and the PGC-1α pathway.

EXPERIMENTAL PROCEDURES

Animals

RAmKO, mTOR$^-$ and PGC1α-TG mice were described earlier (Bentzinger et al., 2008; Lin et al., 2002; Risson et al., 2009). The RAmKO-PGC1α-TG mice were generated by crossing the RAmKO with the PGC1α-TG mice. Mice were maintained in a conventional facility with a fixed light cycle. Body weight was measured weekly. Studies were carried out according to criteria outlined for the care and use of laboratory animals and with approval of the Swiss (for experiments with RAmKO, PGC1α-TG and RAmKO-PGC1α-TG mice) and French authorities (for experiments with mTOR$^-$ mice), respectively.

Quantitative Real-time PCR

Total RNA was isolated (SV Total RNA isolation System, Promega) and equal amounts of RNA reverse transcribed using a mixture of oligodT and random hexamer primers (iScript cDNA Synthesis Kit, Bio-Rad). Quantitative real-time PCR (qRT-PCR) was performed using SYBR Green (Power SYBR Green Master Mix, Applied Biosystems) and StepOne^{TM} Software 2.1. (Applied Biosystems). Expression levels for each gene of interest were normalized to the mean cycle number using qRT-PCR for the housekeeping protein β-actin.

Quantification of mtDNA Copy Numbers

Total DNA was extracted and purified with a standard chloroform/ethanol precipitation after proteinase K digestion. DNA concentrations were determined photometrically, adjusted to 50 ng/µl and used to quantify the amount of mtDNA with respect to the genomic DNA by qRT-PCR. For the quantification of the mtDNA,

primers were used that are complementary to the *D-loop* region. Primers to quantify genomic DNA were directed against the single-copy nuclear gene *Ndufv1*.

Histology

Muscles frozen in liquid nitrogen-cooled isopentane were cut into 12 µm cross-sections. General histology on cross sections was performed using hematoxylin and eosin (H&E, Merck). NADH staining was done as described (Dunant et al., 2003). Periodic acid-Schiff staining (PAS staining system, Sigma) was performed according to the manufacturer's instruction. After all stainings samples were dehydrated and mounted with DePex mounting medium (Gurr, BDH). Succinate dehydrogenase (SDH) and cytochrome oxidase (COX) staining were carried out as described in (Konieczny et al., 2008; MacArthur et al., 2007), respectively.

Statistics

Compiled data are expressed as mean ± SD. One Way Analysis of Variance (ANOVA) and *a priori* defined contrast analysis were performed for statistical comparisons of the different groups. The level of significance is indicated as follows: ***/### $p<0.001$, **/## $p< 0.01$, */# $p< 0.05$.

REFERENCES

Aiston, S., Hampson, L.J., Arden, C., Iynedjian, P.B., and Agius, L. (2006). The role of protein kinase B/Akt in insulin-induced inactivation of phosphorylase in rat hepatocytes. Diabetologia 49, 174-182.

Amthor, H., Macharia, R., Navarrete, R., Schuelke, M., Brown, S.C., Otto, A., Voit, T., Muntoni, F., Vrbova, G., Partridge, T., Zammit, P., Bunger, L., and Patel, K. (2007). Lack of myostatin results in excessive muscle growth but impaired force generation. Proc Natl Acad Sci U S A 104, 1835-1840.

Bastin, J., Aubey, F., Rotig, A., Munnich, A., and Djouadi, F. (2008). Activation of peroxisome proliferator-activated receptor pathway stimulates the mitochondrial respiratory chain and can correct deficiencies in patients' cells lacking its components. J Clin Endocrinol Metab 93, 1433-1441.

Bentzinger, C.F., Romanino, K., Cloetta, D., Lin, S., Mascarenhas, J.B., Oliveri, F., Xia, J., Casanova, E., Costa, C.F., Brink, M., Zorzato, F., Hall, M.N., and Ruegg, M.A. (2008). Skeletal muscle-specific ablation of raptor, but not of rictor, causes metabolic changes and results in muscle dystrophy. Cell Metab 8, 411-424.

Cunningham, J.T., Rodgers, J.T., Arlow, D.H., Vazquez, F., Mootha, V.K., and Puigserver, P. (2007). mTOR controls mitochondrial oxidative function through a YY1-PGC-1alpha transcriptional complex. Nature 450, 736-740.

Dunant, P., Larochelle, N., Thirion, C., Stucka, R., Ursu, D., Petrof, B.J., Wolf, E., and Lochmuller, H. (2003). Expression of dystrophin driven by the 1.35-kb MCK promoter ameliorates muscular dystrophy in fast, but not in slow muscles of transgenic mdx mice. Mol Ther 8, 80-89.

Glass, D.J. (2005). Skeletal muscle hypertrophy and atrophy signaling pathways. Int J Biochem Cell Biol 37, 1974-1984.

Grumati, P., Coletto, L., Sabatelli, P., Cescon, M., Angelin, A., Bertaggia, E., Blaauw, B., Urciuolo, A., Tiepolo, T., Merlini, L., Maraldi, N.M., Bernardi, P., Sandri, M., and Bonaldo, P. (2010). Autophagy is defective in collagen VI muscular dystrophies, and its reactivation rescues myofiber degeneration. Nat Med 16, 1313-1320.

Handschin, C., Chin, S., Li, P., Liu, F., Maratos-Flier, E., Lebrasseur, N.K., Yan, Z., and Spiegelman, B.M. (2007a). Skeletal muscle fiber-type switching, exercise intolerance, and myopathy in PGC-1alpha muscle-specific knock-out animals. J Biol Chem 282, 30014-30021.

Handschin, C., Kobayashi, Y.M., Chin, S., Seale, P., Campbell, K.P., and Spiegelman, B.M. (2007b). PGC-1alpha regulates the neuromuscular junction program and ameliorates Duchenne muscular dystrophy. Genes Dev 21, 770-783.

Konieczny, P., Fuchs, P., Reipert, S., Kunz, W.S., Zeold, A., Fischer, I., Paulin, D., Schroder, R., and Wiche, G. (2008). Myofiber integrity depends on desmin network targeting to Z-disks and costameres via distinct plectin isoforms. J Cell Biol 181, 667-681.

Lin, J., Wu, H., Tarr, P.T., Zhang, C.Y., Wu, Z., Boss, O., Michael, L.F., Puigserver, P., Isotani, E., Olson, E.N., Lowell, B.B., Bassel-Duby, R., and Spiegelman, B.M. (2002). Transcriptional co-activator PGC-1 alpha drives the formation of slow-twitch muscle fibres. Nature 418, 797-801.

MacArthur, D.G., Seto, J.T., Raftery, J.M., Quinlan, K.G., Huttley, G.A., Hook, J.W., Lemckert, F.A., Kee, A.J., Edwards, M.R., Berman, Y., Hardeman, E.C., Gunning,

P.W., Easteal, S., Yang, N., and North, K.N. (2007). Loss of ACTN3 gene function alters mouse muscle metabolism and shows evidence of positive selection in humans. Nat Genet 39, 1261-1265.

Masiero, E., Agatea, L., Mammucari, C., Blaauw, B., Loro, E., Komatsu, M., Metzger, D., Reggiani, C., Schiaffino, S., and Sandri, M. (2009). Autophagy is required to maintain muscle mass. Cell Metab 10, 507-515.

Pederson, B.A., Cope, C.R., Irimia, J.M., Schroeder, J.M., Thurberg, B.L., Depaoli-Roach, A.A., and Roach, P.J. (2005). Mice with elevated muscle glycogen stores do not have improved exercise performance. Biochem Biophys Res Commun 331, 491-496.

Risson, V., Mazelin, L., Roceri, M., Sanchez, H., Moncollin, V., Corneloup, C., Richard-Bulteau, H., Vignaud, A., Baas, D., Defour, A., Freyssenet, D., Tanti, J.F., Le-Marchand-Brustel, Y., Ferrier, B., Conjard-Duplany, A., Romanino, K., Bauche, S., Hantai, D., Mueller, M., Kozma, S.C., Thomas, G., Ruegg, M.A., Ferry, A., Pende, M., Bigard, X., Koulmann, N., Schaeffer, L., and Gangloff, Y.G. (2009). Muscle inactivation of mTOR causes metabolic and dystrophin defects leading to severe myopathy. J Cell Biol 187, 859-874.

Sakamoto, K., and Goodyear, L.J. (2002). Invited review: intracellular signaling in contracting skeletal muscle. J Appl Physiol 93, 369-383.

Sandri, M., Lin, J., Handschin, C., Yang, W., Arany, Z.P., Lecker, S.H., Goldberg, A.L., and Spiegelman, B.M. (2006). PGC-1alpha protects skeletal muscle from atrophy by suppressing FoxO3 action and atrophy-specific gene transcription. Proc Natl Acad Sci U S A 103, 16260-16265.

Tenenbaum, A., Motro, M., and Fisman, E.Z. (2005). Dual and pan-peroxisome proliferator-activated receptors (PPAR) co-agonism: the bezafibrate lessons. Cardiovasc Diabetol 4, 14.

Wende, A.R., Schaeffer, P.J., Parker, G.J., Zechner, C., Han, D.H., Chen, M.M., Hancock, C.R., Lehman, J.J., Huss, J.M., McClain, D.A., Holloszy, J.O., and Kelly, D.P. (2007). A role for the transcriptional coactivator PGC-1alpha in muscle refueling. J Biol Chem 282, 36642-36651.

Wenz, T., Diaz, F., Spiegelman, B.M., and Moraes, C.T. (2008). Activation of the PPAR/PGC-1alpha pathway prevents a bioenergetic deficit and effectively improves a mitochondrial myopathy phenotype. Cell Metab 8, 249-256.

Wu, Z., Puigserver, P., Andersson, U., Zhang, C., Adelmant, G., Mootha, V., Troy, A., Cinti, S., Lowell, B., Scarpulla, R.C., and Spiegelman, B.M. (1999). Mechanisms controlling mitochondrial biogenesis and respiration through the thermogenic coactivator PGC-1. Cell 98, 115-124.

Wullschleger, S., Loewith, R., and Hall, M.N. (2006). TOR signaling in growth and metabolism. Cell 124, 471-484.

ACKNOWLEDGMENTS

Arnaud Ferry from the Université Pierre et Marie Curie-Paris

FIGURE LEGENDS

Figure 1. Increased PGC-1α levels normalize mitochondrial properties in RAmKO mice.

(A) Relative mRNA levels of PGC-1α in EDL muscle of 90-day-old mice as determined by qRT-PCR (n≥3 mice).

(B) Mitochondrial DNA content in EDL muscle of 140-day-old mice. The amount of mtDNA was quantified by qRT-PCR and expressed relative to the amount of nuclear DNA (n≥2 mice).

(C) Relative mRNA levels of the indicated proteins in EDL muscle of 90-day-old mice as determined by qRT-PCR (n≥3 mice). * transgenic mice compared to ctrl mice, # transgenic mice compared to RAmKO mice.

(D) Activity of oxidative enzymes examined by NADH-tetrazolium staining (blue precipitate) in TA muscle of 130-day-old mice. Scale bar = 100μm

(E) Electron micrographs of longitudinal sections of EDL muscle of 140-day-old mice. Scale bar = 200nm.

Individual data points and bars (A, B and C) represent means ± SD. p values are */#p<0.05, **/##p<0.01, ***/###p<0.001.

Figure 2. The glycogen content is increased in all mouse models.

(A) Periodic acid-Schiff (PAS) staining of cross-sections of TA muscle of 90-day-old mice. The reaction product (magenta color) is indicative of amount of glycogen in the tissue. Scale bar = 50μm

(B) Glycogen concentration in the TA muscle from 90-day-old mice.

(C) Western blot analysis of EDL muscle from 80-day-old mice using antibodies directed against the proteins indicated. Equal amount of protein was loaded in each lane. An antibody against α-actinin was used as loading control.

(D) Relative mRNA levels of glycogen phosphorylase in EDL muscle of 90-day-old mice as determined by qRT-PCR (n≥3 mice).

Individual data points and bars (B and D) represent means ± SD. p values are *p<0.05, **p<0.01, ***p<0.001.

Figure 3. Transgenic increase in PGC-1α level does not prevent muscle dystrophy in mice with inactive mTORC1.

(A) Mice of each genotype were weighed every week. RAmKO and RAmKO-PGC1α-TG mice are significantly lighter after the age of 63 days. (n≥5 mice)

(B) Hematoxylin and eosin (H&E) staining of cross-sections of TA muscle of 130-day-old mice. In the muscle of RAmKO and RAmKO-PGC1α-TG mice some large (blue arrows) but also small fibers are present. Both genotypes also show centralized nuclei (white arrows) and many mononuclear cells (green arrows).

(C) Fiber size distribution in the TA muscle of 140-day-old mice. RAmKO and RAmKO-PGC1α-TG mice have significantly (p<0.05) more fibers that have a fiber feret of 20-30μm than control littermates. The amount of fibers with a fiber feret between 40-50μm is significantly reduced in RAmKO mice (p=0.024) and shows a trend towards reduction in RAmKO-PGC1α-TG mice (p=0.064).

(D) Mean percentage of muscle fibers with centralized nuclei (cnf) in TA muscle of 90-day-old mice. (n≥5 mice) Individual data points and bars represent means ± SD.

(E) Average distance run voluntarily per day determined between the age of 95 days and 105 days. (n≥3) Individual data points and bars represent means ± SEM.

(F) Photographs of 140-day-old littermates. The RAmKO and RAmKO-PGC1α-TG mice are leaner and suffer from a kyphosis.

(G) Percentage of mice suffering from kyphosis was determined over several weeks. (n≥7 mice) P values (D and E) are *p<0.05, **p<0.01, ***p<0.001.

Figure 4. Bezafibrate partially restores mitochondrial function in muscles in the absence of mTOR, but does not affect the muscle myopathy.

(A and E) Relative mRNA levels of the indicated proteins in soleus muscle as determined by qRT-PCR (n≥3 mice). Individual data points and bars represent means ± SEM.

(B) Oxidative properties examined by succinate-dehydrogenase (SDH) staining in hind leg muscles. The soleus muscle is marked by an asterisk. Darkly stained fibers contain high SDH activity. Scale bar = 100μm

(C) SDH activity in soleus muscle (n≥5 mice). Individual data points and bars represent means ± SD.

(D) Hematoxylin and eosin (H&E) staining of cross-sections of soleus muscle. In the muscle of $mTOR^-$ and $mTOR^-$ mice treated with bezafibrate some large (blue arrows) but also small fibers are present. Both genotypes also show centralized nuclei (white arrows) and many mononuclear cells (green arrows). Scale bar = 50μm

All mice (A-E) were male and 140 days old. p values (A, C, E) are *p<0.05, **p<0.01, ***p<0.001. * transgenic mice compared to ctrl mice, # transgenic mice compared to $mTOR^-$ mice.

SUPPLEMENTAL DATA

SUPPLEMENTAL TABLES

(1) Weight or length was measured for different organs in 140-day-old mice. (n>6 mice) * transgenic mice compared to ctrl mice, # transgenic mice compared to RAmKO mice.

(2) Muscle contractile properties of 140-day-old mice were assessed by recording isometric forces in response to electrical stimulation. The following data were measured: muscle mass, absolute maximum tetanic force (Po), specific tetanic force (sPo), peak twitch tension (Pt), time taken for maximal twitch tension to fall by 20% (F20%).(n>3 mice) * $mTOR^-$ compared to ctrl mice, # $mTOR^-$ mice compared to $mTOR^-$ mice treated with bezafibrate.

Values for both tables represent means ± SD. P values determined by Student's t test are indicated by asterisks. P values are */#p<0.05, **/##p<0.01, ***/###p<0.001.

SUPPLEMENTAL FIGURES

(A) Relative mRNA levels of PGC-1α in soleus muscle of 90-day-old mice as determined by qRT-PCR (n≥3 mice).Individual data points and bars represent means ± SD. p values are *p<0.05, **p<0.01, ***p<0.001.

(B) Raptor protein amount was determined by Western blot analysis of soleus muscle from 80-day-old mice. Equal amount of protein was loaded in each lane. An antibody against α-actinin was used as loading control.

(C) Photographs of 140-day-old littermates.

(D) Cytochrome oxidase (COX) staining in hind leg muscles. COX is the complex IV of the respiratory chain enzymes and its activity is representative for the oxidative enzymes. The soleus muscle is marked by an asterisk. Scale bar = 100µm

(E) For the qRT-PCR the following primers were used: β-actin (forward: 5' CAG CTT CTT TGC AGC TCC TT, reverse: 5' GCA GCG ATA TCG TCA TCC A). PGC-1α (forward: TGA TGT GAA TGA CTT GGA TAC AGA CA, reverse: GCT CAT TGT TGT ACT GGT TGG ATA TG), PPARα (forward: GCG TAC GGC AAT GGC TTT AT, reverse: ACA GAA CGG CTT CCT CAG GTT), PPARδ (forward: GCA AGC CCT TCA GTG ACA TCA, reverse: CCA GCG CAT TGA ACT TGA CA), MCAD (forward: AAC ACT TAC TAT GCC TCG ATT GCA, reverse: CCA TAG CCT CCG AAA ATC TGA A), Cytochrome C (forward: GCA AGC ATA AGA CTG GAC CAA A, reverse: TTG TTG GCA TCT GTG TAA GAG AAT C), COX IV (forward: TAC TTC GGT GTG CCT TCG A, reverse: TGA CAT GGG CCA CAT CAG), Citrate synthase (forward: CAA GCA GCA ACA TGG GAA GA, reverse: GTC AGG ATC AAG AAC CGA AGT CT), Glycogen phosphorylase (forward: CAC TTA CCA GCT GGG CTT GGA CAT, reverse: AAA GCA AGC TGC CAG GCG TC), COX I (forward: GGT CAA CCA GGT GCA CTT TT, reverse: TGG GGC TCC GAT TAT TAG TG), LCAD (forward: ATG GCA AAA TAC TGG GCA TC, reverse: TCT TGC GAT CAG CTC TTT CA), Dystrophin (forward: TGC GCT ATC AGG AGA CAA TG, reverse: TTC TTG GCC ATC TCC TTC AC), myogenin (forward: CTA CAG GCC TTG CTC AGC TC, reverse: AGA TTG TGG GCG TCT GTA GG), MyH8 (forward: CAA GGA TGG AGG GAA AGT GA, reverse: GGT TCA TGG GGA AGA CTT GA).

(F) For the quantification of mtDNA copy numbers the following primers were used: *D-loop* region (forward: GGT TCT TAC TTC AGG GCC ATC A, reverse: GAT TAG ACC CGT TAC CAT CGA GAT), *Ndufv1* (forward: CTT CCC CAC TGG CCT CAA G, reverse: CCA AAA CCC AGT GAT CCA GC).

SUPPLEMENTAL EXPERIMENTAL PROCEDURES

Electron Microscopy

Transmission electron microscopy was performed as described (Moll et al., 2001).

Western blotting analysis/ Glycogen content/ Fiber size distribution

All three procedures were performed as described earlier (Bentzinger et al., 2008). For Western blots following antibodies were used: Akt, Phospho-Akt (Thr308), Phospho-Akt (Ser473), GSK-3β, Phospho-GSK-3β (Ser9) and Raptor from Cell Signaling, α-actinin from Sigma, GP from Santa Cruz. The concentrations used were according to the manufacturer.

Voluntary wheel running

Mice were individually housed in cages equipped with a running wheel carrying a magnet. Wheel revolutions were registered by a reed sensor connected to an I-7053D Digital-Input module (Spectra), and the revolution counters were read by a standard laptop computer via an I-7520 RS-485-to-RS-232 interface converter (Spectra). Digitalized signals were processed by the "mouse running" software developed by Santhera Pharmaceuticals.

Physiological Studies

Measurements of muscle contractile properties were performed as described (Risson et al., 2009).

Succinate dehydrogenase activity

Muscle samples were homogenized directly from frozen in a stabilizing medium containing 50% glycerol, 20 mM phosphate buffer (pH 7.4), 5 mM β-mercaptoethanol, 0.5 mM EDTA and 0.02% BSA at a dilution of 1:50 based on wet weight. Succinate dehydrogenase activity was determined at 37°C in a two-step assay according to a method adapted from (Chi et al., 1983). In the first step fumarate accumulated from succinate for 60 minutes and in the second step, the fumarate produced was measured with fumarase and a NAD-coupled reaction with malate dehydrogenase and the glutamate-oxaloacetate transaminase. Fluorescence reading of NADH was made after completion of the reaction. Standards were processed the same way as the samples.

REFERENCES

Bentzinger, C.F., Romanino, K., Cloetta, D., Lin, S., Mascarenhas, J.B., Oliveri, F., Xia, J., Casanova, E., Costa, C.F., Brink, M., Zorzato, F., Hall, M.N., and Ruegg, M.A. (2008). Skeletal muscle-specific ablation of raptor, but not of rictor, causes metabolic changes and results in muscle dystrophy. Cell Metab 8, 411-424.

Chi, M.M., Hintz, C.S., Coyle, E.F., Martin, W.H., 3rd, Ivy, J.L., Nemeth, P.M., Holloszy, J.O., and Lowry, O.H. (1983). Effects of detraining on enzymes of energy metabolism in individual human muscle fibers. Am J Physiol 244, C276-287.

Moll, J., Barzaghi, P., Lin, S., Bezakova, G., Lochmuller, H., Engvall, E., Muller, U., and Ruegg, M.A. (2001). An agrin minigene rescues dystrophic symptoms in a mouse model for congenital muscular dystrophy. Nature 413, 302-307.

Risson, V., Mazelin, L., Roceri, M., Sanchez, H., Moncollin, V., Corneloup, C., Richard-Bulteau, H., Vignaud, A., Baas, D., Defour, A., Freyssenet, D., Tanti, J.F.,

Le-Marchand-Brustel, Y., Ferrier, B., Conjard-Duplany, A., Romanino, K., Bauche, S., Hantai, D., Mueller, M., Kozma, S.C., Thomas, G., Ruegg, M.A., Ferry, A., Pende, M., Bigard, X., Koulmann, N., Schaeffer, L., and Gangloff, Y.G. (2009). Muscle inactivation of mTOR causes metabolic and dystrophin defects leading to severe myopathy. J Cell Biol 187, 859-874.

Figure 1

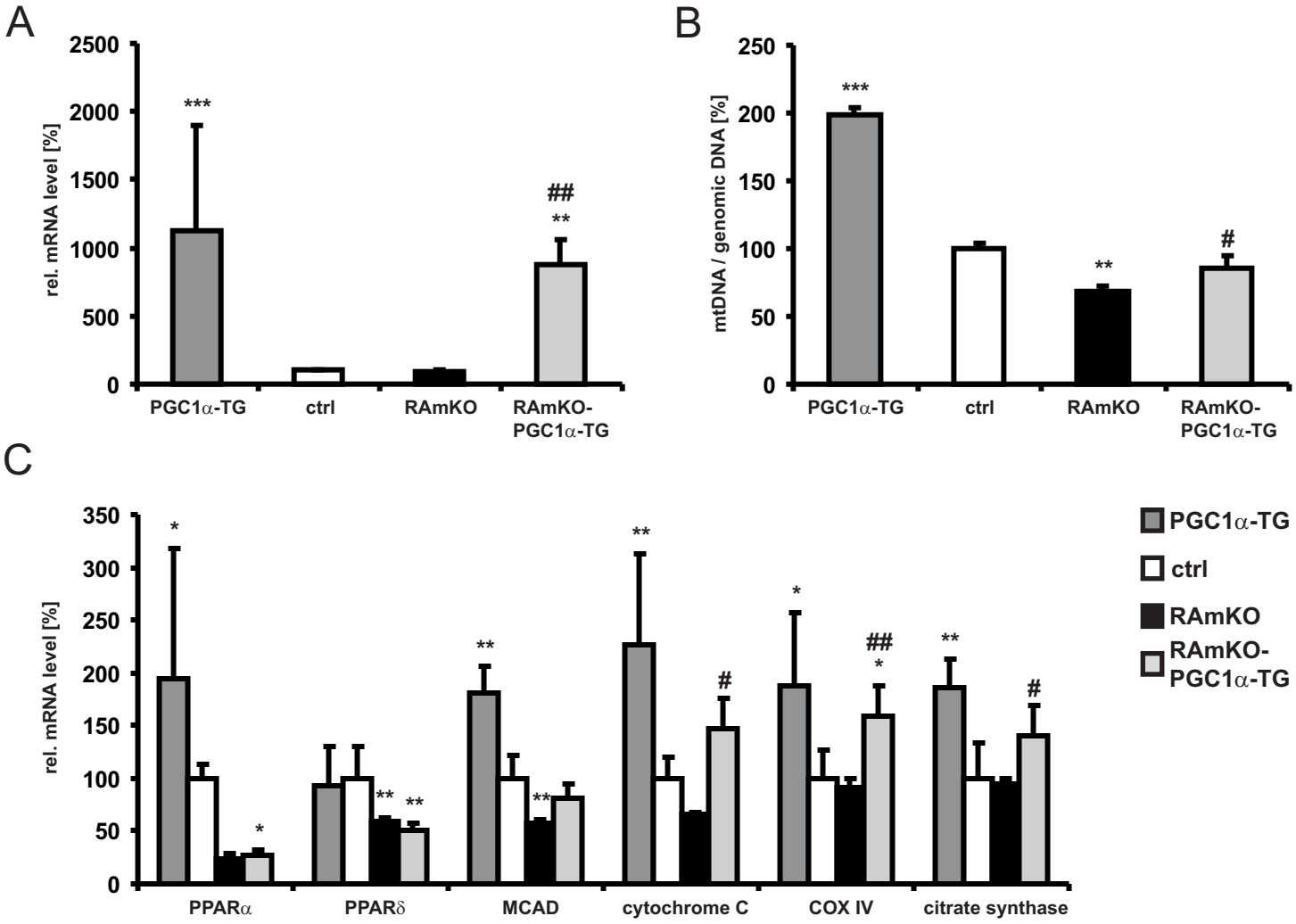
A
rel. mRNA level [%]
2500
2000
1500
1000
500
0
***
**
##
PGC1α-TG
ctrl
RAmKO
RAmKO-PGC1α-TG
B
mtDNA / genomic DNA [%]
250
200
150
100
50
0
***
**
#
PGC1α-TG
ctrl
RAmKO
RAmKO-PGC1α-TG
C
rel. mRNA level [%]
350
300
250
200
150
100
50
0
PPARα
PPARδ
MCAD
cytochrome C
COX IV
citrate synthase
PGC1α-TG
ctrl
RAmKO
RAmKO-PGC1α-TG

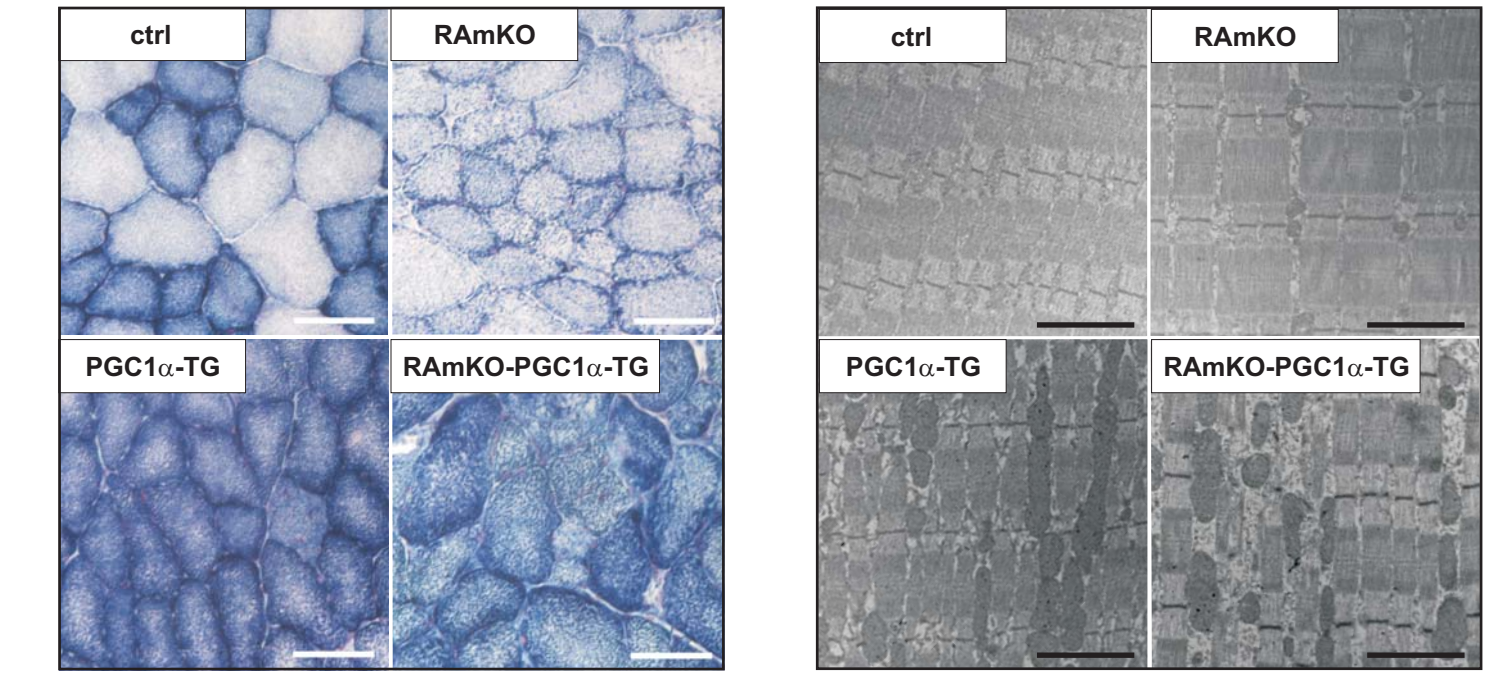
D
ctrl
RAmKO
PGC1α-TG
RAmKO-PGC1α-TG
E
ctrl
RAmKO
PGC1α-TG
RAmKO-PGC1α-TG

Figure 2

A

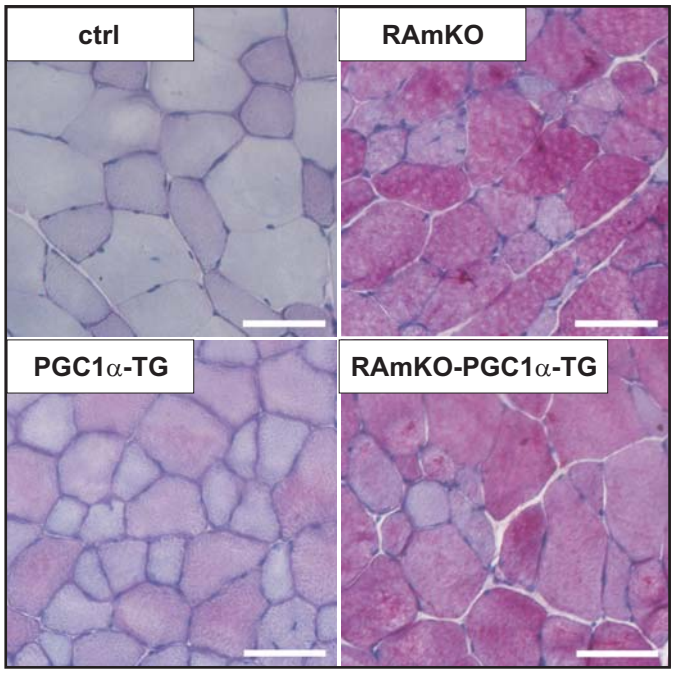

B

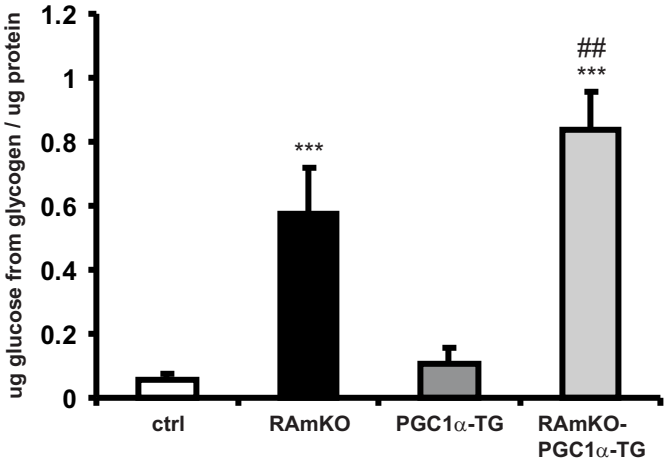

C

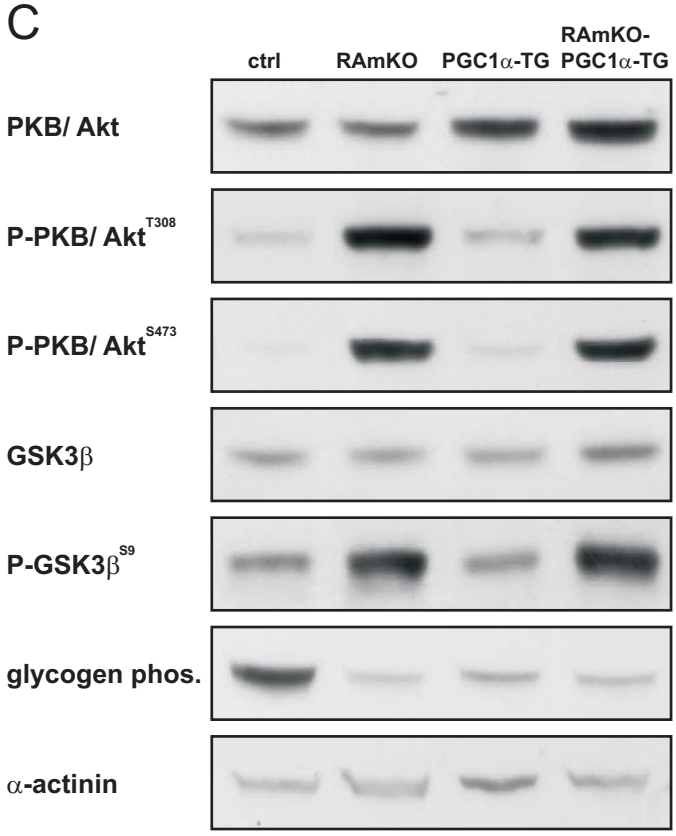

D

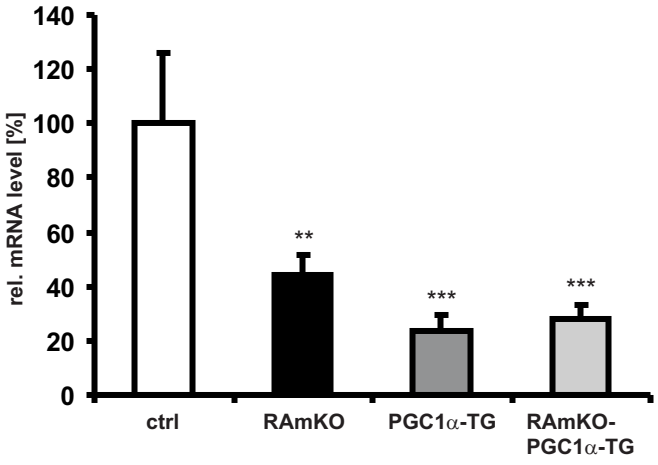

Figure 3

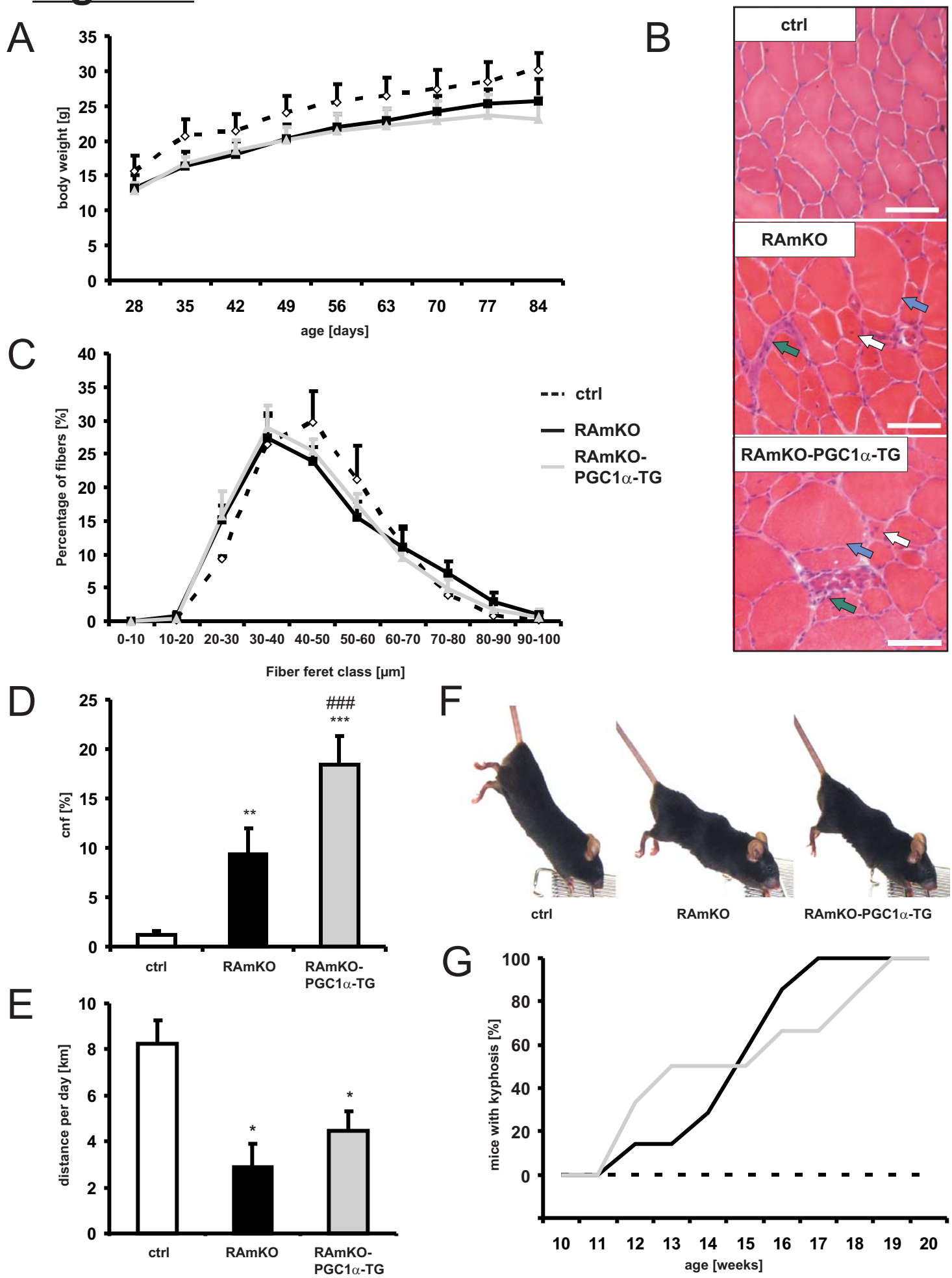
A
body weight [g]
0
5
10
15
20
25
30
35
28
35
42
49
56
63
70
77
84
age [days]
B
ctrl
RAmKO
RAmKO-PGC1α-TG
C
Percentage of fibers [%]
0
5
10
15
20
25
30
35
40
0-10
10-20
20-30
30-40
40-50
50-60
60-70
70-80
80-90
90-100
Fiber feret class [µm]
ctrl
RAmKO
RAmKO-PGC1α-TG
D
cnf [%]
0
5
10
15
20
25
**
###
***
ctrl
RAmKO
RAmKO-PGC1α-TG
E
distance per day [km]
0
2
4
6
8
10
*
*
ctrl
RAmKO
RAmKO-PGC1α-TG
F
ctrl
RAmKO
RAmKO-PGC1α-TG
G
mice with kyphosis [%]
0
20
40
60
80
100
10
11
12
13
14
15
16
17
18
19
20
age [weeks]

Figure 4

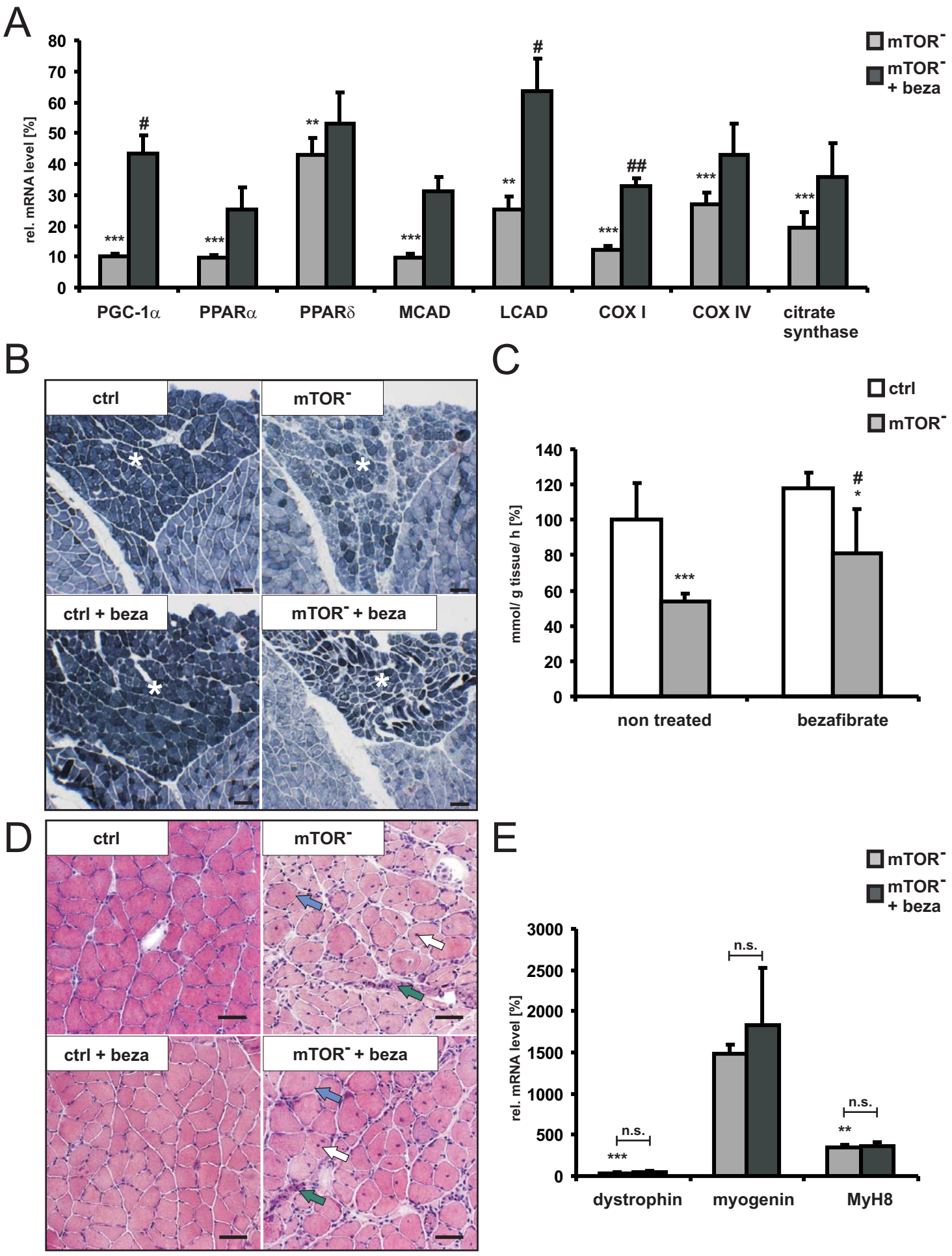
A
rel. mRNA level [%]
mTOR-
mTOR- + beza
PGC-1α
PPARα
PPARδ
MCAD
LCAD
COX I
COX IV
citrate synthase
B
ctrl
mTOR-
ctrl + beza
mTOR- + beza
C
ctrl
mTOR-
mmol/ g tissue/ h [%]
non treated
bezafibrate
D
ctrl
mTOR-
ctrl + beza
mTOR- + beza
E
mTOR-
mTOR- + beza
rel. mRNA level [%]
n.s.
dystrophin
myogenin
MyH8

Supplemental Figure

A

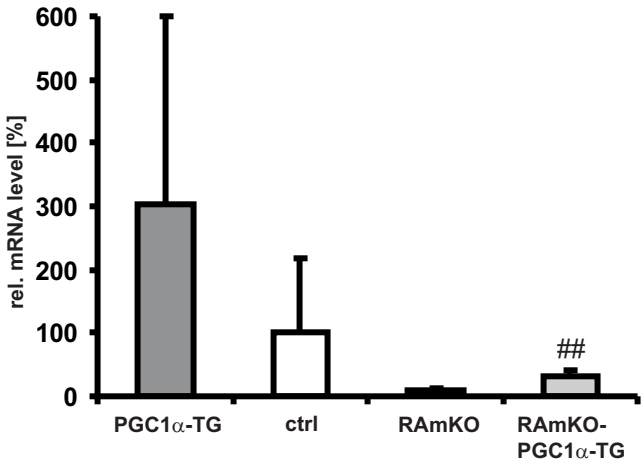

B

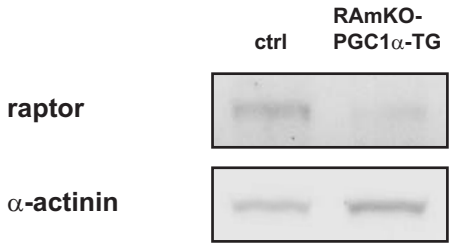

C

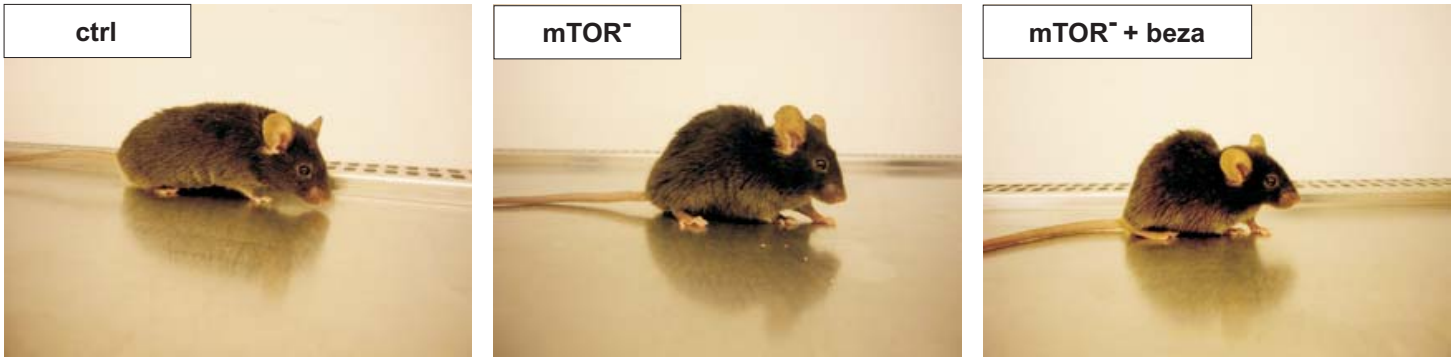

D

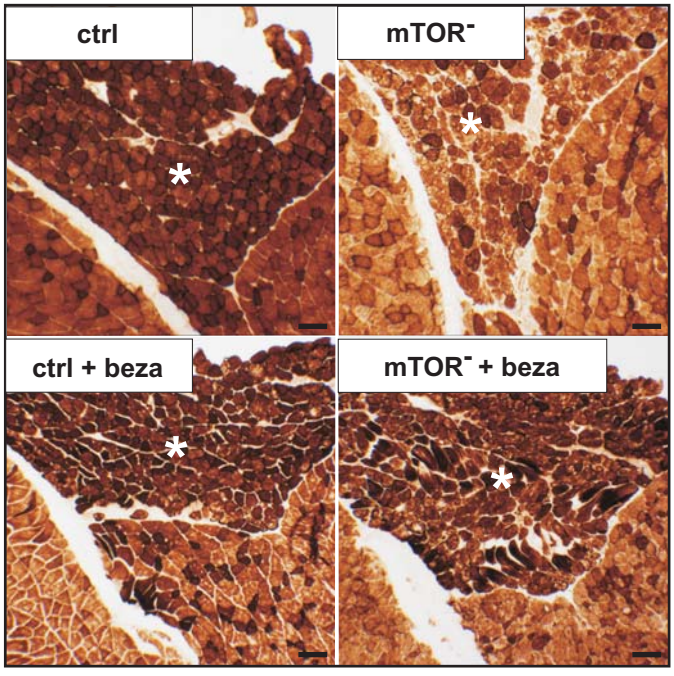

Tables

Table 1

	ctrl	RAmKO	PGC1α-TG	RAmKO-PGC1α-TG
raptor	84 ± 28	4 ± 3*	58 ± 30	2 ± 2*
total Akt	12 ± 3	38 ± 5	46 ± 11*	64 ± 23**
P-Akt T308	15 ± 2	161 ± 7***	17 ± 12	87 ± 0*** #
P-Akt S473	3 ± 3	54 ± 1**	2 ± 1	66 ± 20***
GSK3	34 ± 11	43 ± 1	24 ± 8	47 ± 12
P-GSK3 S9	55 ± 17	111 ± 15*	34 ± 10	101 ± 32*
glycogen phos.	106 ± 24	18 ± 8**	58 ± 31*	22 ± 4**

*p<0.05, **p<0.01, ***p<0.001

Table 2

	ctrl	RAmKO	PGC1α-TG	RAmKO-PGC1α-TG
Soleus (mg)	8.1 ± 0.6	6.6 ± 0.8*	8.6 ± 0.8	6.3 ± 0.6**
EDL (mg)	11.4 ± 1.2	10.6 ± 0.5	11.1 ± 1.3	9.8 ± 1.2
TA (mg)	48.4 ± 3.9	41.8 ± 4.5*	50.9 ± 3.9	35.2 ± 4.4** #
Heart (mg)	147.2 ± 16.4	126.9 ± 4.8	154.8 ± 11.9	136.3 ± 7.9
Liver (mg)	1281.2 ± 338.7	1212.3 ± 139.8	1345.3 ± 140.3	1183.9 ± 161.1
Tibia length (cm)	2.1 ± 0.1	2.1 ± 0.1	2.0 ± 0.1	2.0 ± 0.1

*p<0.05, **p<0.01, ***p<0.001

Table 3

soleus	ctrl	mTOR$^-$	mTOR$^-$ +beza
Mass (mg)	13.2 ± 1.6	9.7 ± 1***	7.0 ± 0.3*** ###
Po (mN)	224.2 ± 52.2	132.0 ± 19.9**	104.8 ± 9.7** #
sPo (mN/mm2)	171.2 ± 40.2	130.6 ± 14.5*	140.0 ± 17.2*
F20%	20.1 ± 6.6	40.0 ± 4.5*	59.1 ± 20.4**
TA			
Mass (mg)	61.5 ± 5.1	38.3 ± 6.9***	26.9 ± 2.3*** ##
Po (mN)	1137.3 ± 118.7	445.8 ± 118.4***	292.3 ± 75.8***
sPo (mN/mm2)	18.5 ± 0.7	11.8 ± 1.1***	11.3 ± 2.4***
Pt (mN)	20.7 ± 3.3	7.2 ± 1.8***	3.3 ± 0.7*** ##
F20%	17.0 ± 1.8	20.6 ± 2.7	24.6 ± 3.6**

*p<0.05, **p<0.01, ***p<0.001